Cent. Eur. J. Chem. • 9(4) • 2011 • 743-749
DOI: 10.2478/s11532-011-0052-4

VERSITA

Central European Journal of **Chemistry**

Thermodynamic description of the Cu–Ni–Pb system

Research Article

Jyrki Miettinen[1], Vania Gandova[2], Spas Georgiev[2], Gueorgui Vassilev[2*]

[1]*Laboratory of Metallurgy, Vuorimiehentie 2K, Helsinki University of Technology, Helsinki FIN-02015, Finland*

[2]*Faculty of Chemistry, University of Plovdiv, 4000 Plovdiv, Bulgaria*

Received 19 January 2011; Accepted 11 April 2011

Abstract: Thermodynamic description is presented for the ternary Cu–Ni–Pb system. Optimized parameters of the sub-systems, Cu–Ni, Cu–Pb and Ni–Pb, are taken from earlier assessments and those of the ternary system are optimized in this study by using the experimental phase equilibrium and thermodynamic data. Better agreement is obtained by the present optimization. Calculated results are compared with the original experimental data to demonstrate the successfulness of this assessment. Moreover, a geometric model (general solution model) is used to estimate ternary integral molar Gibbs excess energies of the liquid phase from the bibary systems only. These values, however, disagree with the quantities obtained by thermodynamic optimizations.

Keywords: *Cu–Ni–Pb system • Thermodynamic optimization • General solution model • Substitutional solution model*

1. Introduction

Copper and nickel are among the most often used metals for metallization in electronic devices and are expected to take part of new multicomponent solders. For example, a thermodynamic database comprising 11 selected elements (Cu, Ni, Sn, Pb *etc.*) and the respective binary and ternary systems [1] was recently developed. Moreover, copper-nickel based alloys, are famous for their corrosion resistance and working properties (e.g. for heat-exchangers and corrosive fluid containers). Such alloys (based on Ni–Pb, Cu–Pb and Cu–Ni–Pb systems) have found use as bearings in heavy-duty diesel engines. Besides, the present study continues the recently started work for the development of a thermodynamic database for technically important copper-lead alloys containing Cu, Ni, Sn, Pb, Zn *etc.* [2–7]. The accessibility of thermodynamic descriptions allows also calculating some physical properties (*e.g.* surface tension, viscosity) and predicting the solidification kinetics of the corresponding alloys. The interest to these materials is confirmed by the efforts to create a thermodynamic database for multicomponent solders and copper-base alloys by the group of Ishida [8–10].

Earlier experimental studies on the ternary Cu–Ni–Pb system have been reviewed in [11]. Bierlein and Deltart [12] have shown that the effectiveness of Cu–Ni–Pb bearing materials is strongly related to the phase equilibria in that system. That is why they deserve a better elucidation.

Thus Guertler and Menzel [13] investigated by thermal analyses and metallographic methods an isopleth section having a mass ratio Cu *vs.* Ni equal to 1 *vs.* 3 as well as a section with constant Pb content of 6 wt.%. They observed demixing in the central part of the ternary phase diagram. The miscibility gap disappeared in Ni–Pb samples alloyed with 6 wt.% Cu, while in Cu–Pb specimens it disappeared when adding 2.5 wt.% Ni. Detailed investigations of the ternary system Cu–Ni–Pb were performed later by Nemilov and Strunina [14] by means of thermal analyses, microstructure observation and Brinel-hardness measurements. Three isopleth sections having mass ratios Cu *vs.* Ni equal to 1/1, 4/1 and 1 *vs.* 2, as well as two sections with constant Pb contents of 60 at.%, and 30% at.% were constructed. Later Pelzel [15] reported thermal analysis results for the Cu–Ni, Ni–Pb and the Cu–Ni–Pb systems. Alloys containing 50, 60, 70 and 80 wt.% Pb were studied in the latter system. More recently Szkoda [16] synthesized and

* *E-mail: gpvassilev@uni-plovdiv.bg*

studied seven ternary alloys at various temperatures by means of X-ray and metallographic techniques.

Although thermodynamic data for the liquid phase are available [11,14,17] they are not exhaustive. Nevertheless, the so called "geometric models" give the possibility to assess the thermodynamic properties of a ternary liquid phase, by means of data originating from the respective binary border systems [18–23].

Therefore, the purpose of this work was to compare ternary liquid phase descriptions obtained by the prominent geometric "general solution model" (GSM) [22,23]) to the results achieved by thermodynamic optimizations. The Cu–Ni–Pb system has earlier been assessed by [24]. Nevertheless the latter description could not be adapted directly to the copper-lead alloys thermodynamic database. The reason is that different binary thermodynamic data (particularly for the Cu–Pb system) were used in [24] and in this work. That is why a new description consistent with the latter database was necessary.

2. Phases and Models

The integral molar excess Gibbs energy (ΔG^E_{123}, J mol^{-1}) of a ternary phase (in this case – liquid), consisting of the elements 1, 2 and 3 with mole fractions X_j, is given by the expression:

$$\Delta G^E_{123} = X_1 X_2 \Delta G^E_{12} + X_2 X_3 \Delta G^E_{23} + . \\ + X_3 X_1 \Delta G^E_{31} + \Delta G^{E,ternary} \quad (1).$$

$\Delta G^E_{i,j}$ represent the respective values for the two-component liquid phases, where the down indexes indicate the considered binary system, and $\Delta G^{E,ternary}$ is the contribution of the ternary non-ideal mixing.

The geometric models allow to forecast the thermodynamic properties of a ternary phase (*e.g.* – liquid) using data belonging to the relevant binary end-systems (see Eq. 1). Values of the molar excess Gibbs energies for each binary liquid phase of the border-system (at a certain temperature and at specific compositions) are needed as starting points for the GSM [22,23]. These quantities were calculated by means of Thermocalc software package, using optimized parameters of the pertinent binary systems, recently selected as result of the European concerted action COST 531 [1]. The general solution model allows assessing $\Delta G^{E,ternary}$ using Eq. 2:

$$\Delta G^{E,ternary} = X_1 X_2 X_3 f_{123} \quad (2)$$

where f_{123} is a calculated ternary interaction parameter.

Details about the application of the GSM have already been discussed in a variety of studies (*e.g.* [25–27]) as well as in recent works of the present authors [28,29]. That is why they shall not be discussed further.

A number of thermodynamic optimizations of the Cu–Pb system have been published [30–33] but new experimental results on the liquid phase miscibility gap have become known afterward [34]. The latter data differs considerably from those, reported beforehand.

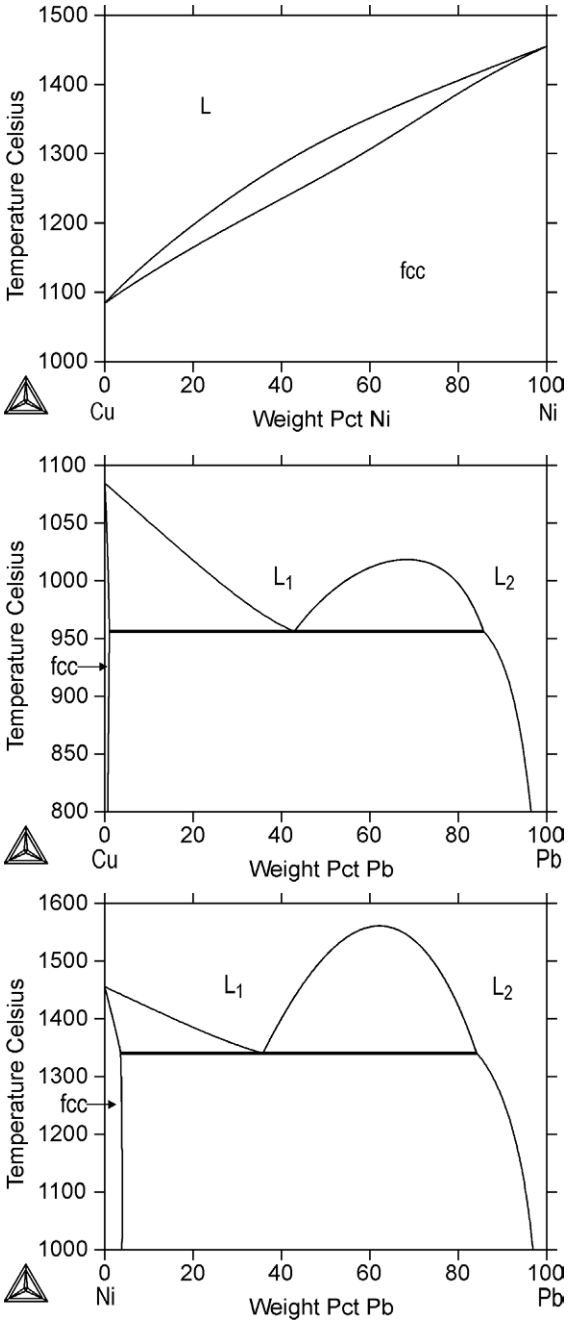

Figure 1. Calculated phase diagrams of binaries Cu-Ni (a), Cu-Pb (b) and Ni-Pb (c) up to [36], [37] and [24], respectively.

Also, discrepancies are observed in the literature concerning the descriptions of the binary systems related to the Cu–Pb–Ni equilibrium diagram. Regarding the Cu–Pb system, the optimization of Hayes *et al.* [30] was retained in the thermodynamic database of COST 531 [1] (*i.e.*, the results of Wang *et al.* [24] were not used. The optimization of the Cu–Ni system done by Mey [35] was retained by both - Wang *et al.* [24] and COST 531 database [1]. The Ni–Pb system was optimized by Wang *et al.* [24] and their parameters were preserved by COST 531 database [1].

Table 1 shows the type of the experimental information selected in the present optimization. Most experimental data comes from Nemilov ang Strunina [14] and Pelzel [15]. No ternary solid phases have been reported to exist in the Cu–Ni–Pb system. The study of Nemilov and Strunina [14] covered the whole system, however quite few data points were presented. Close to the Cu–Pb side of the system, these data were slightly inconsistent with the data of Pelzel [15], who presented numerous data points in this region. Consequently, the latter data [15] were preferred near the Cu–Pb side of the system.

Figs. 1a,b,c show calculated phase diagrams for binaries Cu–Ni [36], Cu–Pb [37] and Ni–Pb [24], respectively. They agree well with the experimental phase equilibrium data as presented in these studies.

As it is generally accepted [11] two liquid miscibility gaps exist, near the Cu–Pb and Ni–Pb sides, but they extend only a little into the ternary system. The main solid phase is fcc (face-centered cubic nickel). In fact, in the Cu–Ni–Pb system, no other solid phases have been reported to exist. Thus, in the present description, only two phases are considered, *i.e.*, liquid and fcc. These disordered solution phases are described with the substitutional solution model.

By applying the substitutional solution model to the solution phases of the Cu–Ni–Pb system, the expression for the integral molar Gibbs energy (G_m^{ϕ}, J mol^{-1}) becomes

$$G_m^{\phi} = x_{Cu}^{\phi}\,{}^{o}G_{Cu}^{\phi} + x_{Ni}^{\phi}\,{}^{o}G_{Ni}^{\phi} + x_{Pb}^{\phi}\,{}^{o}G_{Pb}^{\phi} + RT(x_{Cu}^{\phi}\ln x_{Cu}^{\phi} + x_{Ni}^{\phi}\ln x_{Ni}^{\phi} + x_{Pb}^{\phi}\ln x_{Pb}^{\phi}) + x_{Cu}^{\phi}x_{Ni}^{\phi}L_{Cu,Ni}^{\phi} + x_{Cu}^{\phi}x_{Pb}^{\phi}L_{Cu,Pb}^{\phi} + x_{Ni}^{\phi}x_{Pb}^{\phi}L_{Ni,Pb}^{\phi} + x_{Cu}^{\phi}x_{Ni}^{\phi}x_{Pb}^{\phi}L_{Cu,Ni,Pb}^{\phi} + {}^{mo}G_m^{\phi} \quad (3)$$

where the contribution to the Gibbs energy due to the magnetic ordering, ${}^{mo}G_m^{\phi}$, is expressed as

$${}^{mo}G_m^{\phi} = RT\ln(\beta^{\phi}+1)\cdot f(\tau) \quad (4)$$

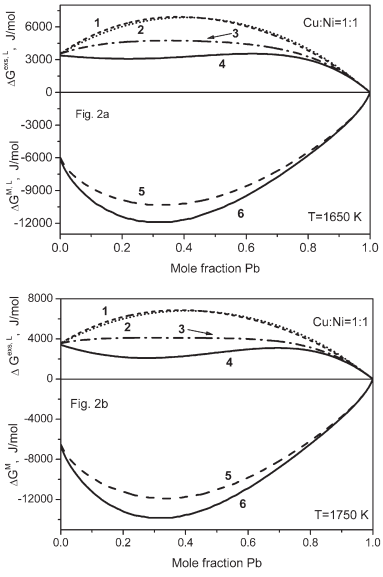

Figure 2. Integral molar Gibbs excess energies ($\Delta G^{exs,L}$, J mol^{-1}) of the ternary liquid phase calculated (at 1650 K and 1750 K, respectively) along a section with constant molar Cu/Ni ratio equal to 1/1. Curve 1 is calculated using binary optimizations of COST 531 thermodynamic database [1], curve 2 – using GSM [22], curve 3 – ternary optimization of Wang *et al.* [24], curve 4 – this work. Curve nos. 5 and 6 compare the integral molar Gibbs energy $\Delta G^{M,L}$, J mol^{-1} (referred to the liquid state) assessed using ternary optimized parameters of Wang *et al.* [24] and this work, respectively.

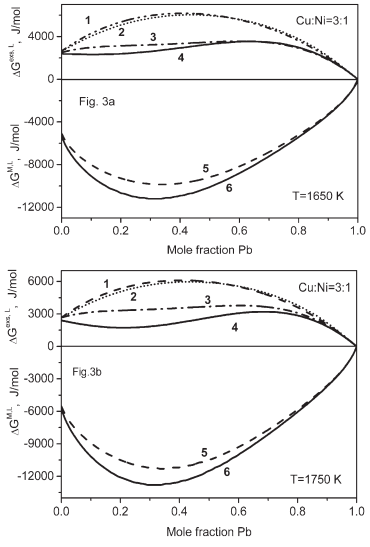

Figure 3. Integral molar Gibbs excess energies ($\Delta G^{exs,L}$, J mol^{-1}) of the ternary liquid phase calculated (at 1650 K and 1750 K, respectively) along a section with constant molar Cu/Ni ratio equal to 3/1. Curve 1 is calculated using binary optimizations of COST 531 thermodynamic database [1], curve 2 – using GSM [22, 23], curve 3 – ternary optimizations of Wang *et al.* [24], curve 4 – this work. Curve nos. 5 and 6 show the integral molar Gibbs energy $\Delta G^{M,L}$, J mol^{-1} (referred to the liquid state) assessed using ternary optimized parameters of Wang *et al.* [24] and this work, respectively.

Table 1. Experimental information applied in the optimization process.

Experimental information type	Reference
Liquidus surfaces	[14, 15]
Cu-Pb side monovriant curve (L_1+L_2 region)	[15]
Ni-Pb side monovriant curve (L_1+L_2 region)	[13, 16]
Liquidus temperatures of Cu-Pb rich ternary alloys	[15]
Isopleth at 60 wt% Pb	[14, 15]
Two isopleths, at wt% Cu:wt% Ni = 1 and 3	[14, 17]

Table 2. Thermodynamic data for the Cu-Ni-Pb system obtained from the literature (reference code) and optimized (*O) or estimated (*E) in this study. All parameter values are in J mol^{-1} of atoms. The thermodynamic data of the pure components are taken from Dinsdale [38] unless a parameter expression is shown in the Table.

Phase	Sublattice description	Reference
Liquid	1 sublattice, sites: 1, constituents: Cu,Ni,Pb	
Parameters	Values	
$L^{L}_{Cu,Ni}$	$(11760+1.084T) + (-1672)(x_{Cu}-x_{Ni})$	[36]
$L^{L}_{Cu,Pb}$	$(31008-7.195T) + (15345-10.826T)(x_{Cu}-x_{Pb}) + (-6493+5.947T)(x_{Cu}-x_{Pb})^2 + (-18416+13.16T)(x_{Cu}-x_{Pb})^3$	[37]
$L^{L}_{Ni,Pb}$	$(31532-2.425T) + (10460-2.498T)(x_{Ni}-x_{Pb}) + (-10927+7.952T)(x_{Ni}-x_{Pb})^2 + (-3732-0.109T)(x_{Ni}-x_{Pb})^3$	[24]
$L^{L}_{Cu,Ni,Pb}$	$(210000-200T)x_{Cu} + (515000-340T)x_{Ni} + (210000-200T)x_{Pb}$	*O
fcc	1 sublattice, sites: 1, constituents: Cu,Ni,Pb	
Parameters	Values	
$L^{fcc}_{Cu,Ni}$	$(8366+2.802T) + (-4360+1.812T)(x_{Cu}-x_{Ni})$	[36]
$L^{fcc}_{Cu,Pb}$	$+45684+5.151T$	[37]
$L^{fcc}_{Ni,Pb}$	$(29980+0.59T) + (-20000+25T)(x_{Ni}-x_{Pb})$	[24]
$L^{fcc}_{Cu,Ni,Pb}$	$+100000$	*O
bcc	1 sublattice, sites: 1, constituents: Cu,Ni,Pb	
Parameters	Values	
$L^{bcc}_{Cu,Ni}$	$+8366+2.802T$	[36]
$L^{bcc}_{Cu,Pb}$	$L^{bcc}_{Cu,Pb} = L^{fcc}_{Cu,Pb}$ (bcc not stable in binary Cu-Pb)	*E
$L^{bcc}_{Ni,Pb}$	$L^{bcc}_{Ni,Pb} = L^{fcc}_{Ni,Pb}$ (bcc not stable in binary Ni-Pb)	*E
Cu_3Sn (ε)	2 sublattices, sites: 0.75:0.25, constituents: Cu:Sn	
Parameters	Values	
${}^{o}G^{\varepsilon}_{Cu:Sn}$	$0.750{}^{o}G^{fcc}_{Cu} + 0.250{}^{o}G^{bct}_{Sn} + (-8218-0.18T)$	03Mie

(*) The lattice stabilities of the pure elements in the gamma phase are related to fcc_A1 of Cu and BCT_Sn, according to the treatment of [98Lia], though the ordered structure of the Cu-Sn gamma phase is supposed to be B2_BCC.

In Eq. 3, R is the gas constant (8.3145 J (K mol)$^{-1}$), T is the absolute temperature, K, x_i is mole fraction of the constituent *i*. ${}^{o}G^{\varphi}_{i}$ is the integral molar Gibbs energy of pure component *i* in phase *φ,* relative to the enthalpy of the same component in its stable state at 298.15 K [38], $L^{\varphi}_{i,j}$ is a binary parameter describing the interaction between components *i* and *j* in the phase φ, and $L^{\varphi}_{Cu,Ni,Pb}$ is a ternary interaction parameter of phase φ. For these parameters, ${}^{o}G^{\varphi}_{i}$ is a function of temperature, and $L^{\varphi}_{i,j}$ and $L^{\varphi}_{Cu,Ni,Pb}$ can be functions of temperature and composition.

In Eq. 4, β^{φ} is a composition-dependent parameter related to the total magnetic entropy and τ is defined as $\tau=T/Tc^{\varphi}$ where Tc^{φ} is the critical temperature of magnetic ordering. For the fcc phase, the function $f(\tau)$ takes the polynomial form proposed by Hillert and Jarl [39]. For the liquid phase, ${}^{mo}G_{m}{}^{\varphi} = 0$.

3. Results and Discussion

The thermodynamic description of the Cu–Ni–Pb systems obtained in this work is presented in Table 2. The data marked with a reference code were adopted from assessments and the data marked with *O or *E were optimized or estimated in the present study. Parameter marked by *O were optimized using literature experimental data (Table 1) while these denoted by *E, were estimated arbitrarily, by applying no experimental data. The thermodynamic data for the pure components are given by Dinsdale [38]. The magnetic ordering parameters for the fcc phase are given as $\beta^{fcc}=0.52x_{Ni}+(x_{Cu}-x_{Ni})(-0.732-0.317(x_{Cu}-x_{Ni}))$, $T_C{}^{fcc}=633x_{Ni}+(x_{Cu}-x_{Ni})(-935.5-549.9(x_{Cu}-x_{Ni}))$ $\beta^{bcc}=0.85x_{Ni}$ [36,38].

Integral molar Gibbs excess energies ($\Delta G^{exs,L}$, J mol^{-1}) of the ternary liquid phase, along sections with constant molar Cu/Ni ratios equal to 1/1 and 3/1, calculated (at 1650 K and 1750 K, respectively) by various models are presented in Figs. 2a,b and 3a,b, respectively. Values of the integral molar Gibbs energy $\Delta G^{M,L}$, J mol^{-1} (at the same conditions) assessed using ternary optimized parameters of this work and of Wang *et al.* [24] are exhibited in these figures as well. In all cases, the $\Delta G^{exs,L}$ values are positive as it should be expected taking into account the formation of the miscibility gaps in the ternary system. The quantities calculated using GSM [22,23] and these obtained by using optimized parameters of the binary systems [1] are rather alike to each other (see curves 1 and 2). The results obtained with the parameters of Wang *et al.* [24] (curves 3 and 5) are near to these obtained in this work (curves 4 and 6). It could be concluded that the GSM did not lead to correct values of the ternary integral molar Gibbs excess energies. This might be related to a hypothetical common drawback of GSM. Thus, in the case of three ideal binary solutions (i-j, i-k and j-k) the assessed ternary (i-j-k) integral molar Gibbs excess energy is par excellence equal to zero what the case might not be.

In the following, calculated results are compared with the original experimental data to demonstrate the successfulness of the optimization. All calculations were carried out with the ThermoCalc software [40]. Thus Fig. 4 shows the liquidus surfaces of the Cu–Ni–Pb system calculated in this study and in the earlier assessment [24]. The agreement with the experimental data [13–16] is reasonably good in both cases. The main difference in the results of the optimizations is the better consistency of the present calculations for the Ni–Pb side L_1+L_2 region (Fig. 4a, two data points at $x_{Pb}=0.3$ from [16] and [13]) and for the isotherms at 1000 and 980°C close to the Cu–Pb side (Fig. 4b). The ternary extension of the Cu–Pb side L_1+L_2 region is better described in [24] (Fig.4b) but its overall area (in composition) is smaller than that shown by the experimental data and obtained by the present assessment. Note also the different form of the calculated isotherms at 930°C. The present, more curved shape of that isotherm is supported by the diagram proposed by [17] though its information below 1000°C should be considered only tentative.

Fig. 5 shows the calculated liquidus temperatures for Cu–Pb rich ternary alloys. Also in this case, better agreement is obtained by the present calculations.

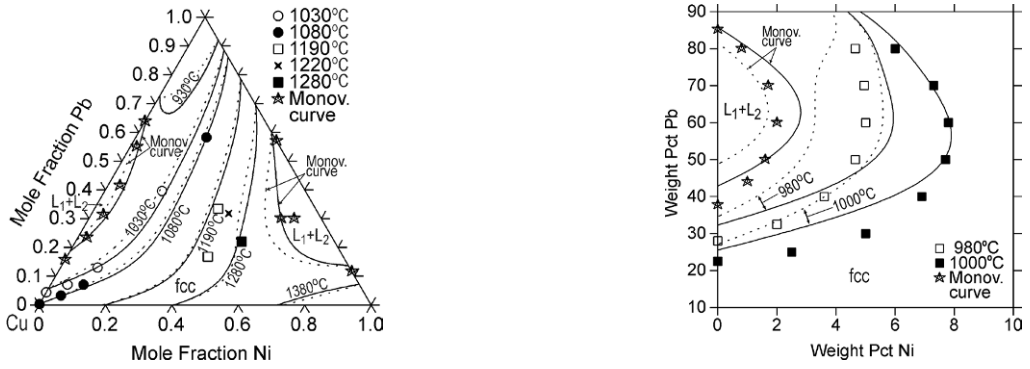

Figure 4. Calculated liquidus surfaces of the Cu-Ni-Pb system (a) and an enlarged section from the Cu-Pb side, together with experimental data points [13–16]. In Fig. 4b, the experimental data points are from the smoothed experimental data of Pelzel [15]. Solid lines refer to the calculations of this study and dashed lines refer to those of [24].

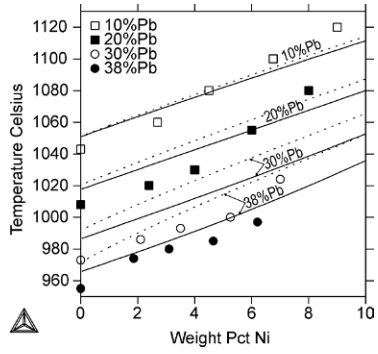

Figure 5. Calculated liquidus temperatures of Cu-Ni-Pb alloys at low nickel contents, together with experimental data points [15]. Solid lines refer to the calculations of this study and dashed lines refer to those of [24].

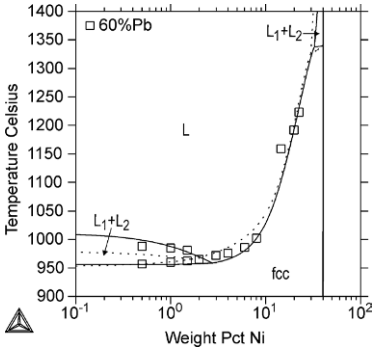

Figure 6. Calculated isopleth of the Cu-Ni-Pb system at 60 wt% Pb, together with experimental data points [14,15]. Solid lines refer to the calculations of this study and dashed lines refer to those of [24].

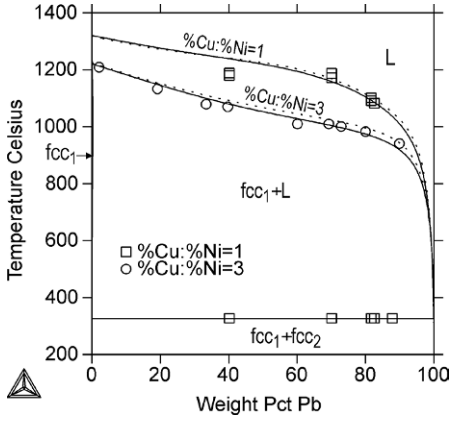

Figure 7. Calculated isopleths of the Cu-Ni-Pb system at composition ratios of wt%Cu / wt%Ni=1 and wt%Cu / wt%Ni=3, together with experimental data points [14,15]. Solid lines refer to the calculations of this study and dashed lines refer to those of [15].

This is mainly due to the heavy weight put on the data of Pelzel [15], whereas Wang *et al.* [24] put the most weight on the data in [17].

The calculated isopleth at 60 wt% Pb is presented in Fig. 6. Worth noting is the larger temperature range of the Cu–Pb side (L_1 + L_2) region obtained by the present calculations. This agrees reasonably well with the experimental data of Pelzel [15]. The higher temperature obtained for the L/L_1+L_2 boundary is due to the adopted Cu–Pb description of Onderka and Zabdir [37], which slightly overestimates its value in the binary Cu–Pb system. For the monotectic reaction, L_1 = fcc + L_2, however, it gives very good agreement with the available experimental data (compare the calculations with the experimental monovariant points at the Cu–Pb side of Fig. 1b).

Finally, Fig. 7 shows two calculated isopleths, at composition ratios of wt% Cu : wt% Ni =1, and wt% Cu: wt% Ni = 3. Both isopleths agree reasonably well with the experimental data [14,17].

4. Conclusions

Thermodynamic descriptions were reoptimized for the ternary Cu–Ni–Pb system applying the experimental phase equilibrium data of the literature. Only two phases, *i.e.*, liquid and fcc, were considered. These disordered solution phases were described with the substitutional solution model. In the optimization, the unary and binary thermodynamic data of the systems were taken from the recently assessed optimizations. Reasonable correlation was obtained between the calculated and experimental phase equilibrium data.

The general solution model was used to assess ternary integral molar Gibbs excess energies of the liquid phase. The latter disagree clearly with the values obtained by the ternary system optimizations. This might indicate a potential drawback of GSM when dealing with ideal solutions (as is approximately the case of Cu–Ni system).

Acknowledgement

This work is related to the European concerted action COST MP 0602 "Advanced Solder Materials for High Temperature Application (HISOLD)".

References

[1] A. Dinsdale, A. Watson, A. Kroupa, J. Vrestal, A. Zemanova, J. Vizdal, Atlas of Phase Diagrams for the Lead-Free Soldering, COST 531 (Lead-free Soders), (© COST office, Czech Republic, 2008) Vol. 1, ISBN 978-80-86292-28-1
[2] J. Miettinen, CALPHAD 27, 263 (2003)
[3] J. Miettinen, CALPHAD 27, 309 (2003)
[4] J. Miettinen, CALPHAD 29, 40 (2005)
[5] J. Miettinen, CALPHAD 29, 212 (2005)
[6] J. Miettinen, V. Gandova, G. Vassilev, CALPHAD 34, 377 (2010)
[7] J. Miettinen, P. Docheva, G. Vassilev, CALPHAD 34, 415 (2010)
[8] X.J. Liu, I. Ohnuma, C.P. Wang, M. Jiang, R. Kainuma, K. Ishina, M. Ode, T. Koyama, H. Onodera, T. Suzuki, J. Electron. Mater. 32, 1265 (2003)
[9] C.P. Wang, X.J. Liu, M. Jiang, I. Ohnuma, R. Kainuma, K. Ishida, J. Phys. Chem. Solids 66, 256 (2005)
[10] M. Jiang, C.P. Wang, X.J. Liu, I. Ohnuma, R. Kainuma, G.P. Vassilev, K. Ishida, J. Phys. Chem. Solids 66, 246 (2005)
[11] Y.A. Chang, J.P. Neumann, A. Mikula, D. Goldberg, INCRA Monograph VI, (1979)
[12] J.C. Bierlein, A.O. Deltart, SAE Tech. Paper Series No. 836064, 1 (1983)
[13] W. Guertler, F. Menzel, Z. Metallkd. 15, 223 (1923) (In German)
[14] V.A. Nemilov, T.A. Strunina, Zhurnal Prikladnoi Khimii 19, 449 (1946) (In Russian)
[15] E. Pelzel, Metall 11, 667 (1957) (In German)
[16] F. Szkoda, Zesz. Nauk. Politech. Czestochow. Metal. 13, 71 (1968) (In Polish)

[17] F. Guertler, Z. Menzel, Anorg. Allgem. Chemie 132, 201 (1924)
[18] F. Kohler, Monatshefte fur Chemie 91, 738 (1960)
[19] Y-M. Muggianu, M. Gambino, J.P. Bros, Journal de Chimie Physique 72, 83 (1975) (In French)
[20] G.W. Toop, Transactions of the American Institute of Mining Engineers 233, 850 (1965)
[21] M. Hilert, CALPHAD 4, 1 (1980)
[22] K.C. Chou, CALPHAD 19, 315 (1995)
[23] K.C. Chou, W.C. Li, F. Li, M. He, CALPHAD 20, 395 (1996)
[24] C. Wang, X. Liu, I. Ohnuma, R. Kainuma, K. Ishida, CALPHAD 24, 149 (2000)
[25] D. Živković, Ž. Živković, Y. Liu, Journal of Alloys and Compounds 265, 176 (1998)
[26] D. Živković, Ž. Živković, J. Šestak, CALPHAD 23, 113 (1999)
[27] D. Manasijević, D. Živković, Ž. Živković, CALPHAD 27, 361 (2003)
[28] N. Milcheva, J. Romanowska, G. Vassilev, Cent. Eur. J. Chem. 9, 149 (2011)
[29] V. Gandova, J. Romanowska, G. Vassilev, RMZ-Materials & Geoenvironment 57, 441 (2010)
[30] F.H. Hayes, H.L. Lukas, G. Effenberg, G. Petzow, Z. Metallkd. 77, 749 (1986)
[31] J. Niemel, G. Effenberg, K. Hack, J. Spencer, CALPHAD 10, 77 (1986)
[32] O. Teppo, J. Niemela, P. Taskinen, Thermochim. Acta 185, 155 (1991)
[33] W.J. Boettinger, C.A. Handwerker, U.R. Kattner, In: F.G. Yost, F.M. Hosking, D.R. Frear (Eds.), The Mechanics of Solder Alloy Wetting and Spreading (Van Nostrand Reinhold, New York, 1993) 103
[34] R.A. Khairulin, S.V. Stankus, Journal of Phase Equilibria 20, 148 (1999)
[35] S. Mey, CALPHAD 16, 255 (1992)
[36] Å. Jansson, TRITA-MAC-0340 (Materials Research Centre, Royal Institute of Technology, Stockholm, 1987)
[37] B. Onderka, L. Zabdyr, Scand. J. Metall. 30, 320 (2001)
[38] A.T. Dinsdale, CALPHAD 15, 317 (1991)
[39] M. Hillert, M. Jarl, CALPHAD 2, 227 (1978)
[40] B. Sundman, B. Jansson, J-O. Andersson, CALPHAD 9, 153 (1985)